Author Manuscript

Author Manuscript

Author Manuscript

Author Manuscript

HHS Public Access

Author manuscript

Biochemistry. Author manuscript; available in PMC 2017 September 13.

Published in final edited form as:

Biochemistry. 2016 September 13; 55(36): 5061–5072. doi:10.1021/acs.biochem.6b00630.

Molecular Interactions of Lipopolysaccharide with an Outer Membrane Protein from *Pseudomonas aeruginosa* Probed by Solution NMR

Iga Kucharska, **Binyong Liang**, **Nicholas Ursini**, and **Lukas K. Tamm***

Center for Membrane and Cell Physiology and Department of Molecular Physiology and Biological Physics, University of Virginia School of Medicine, Charlottesville, Virginia 22908, United States

Abstract

Pseudomonas aeruginosa is an opportunistic human pathogen causing pneumonias that are particularly severe in cystic fibrosis and immunocompromised patients. The outer membrane (OM) of *P. aeruginosa* is much less permeable to nutrients and other chemical compounds than that of *Escherichia coli*. The low permeability of the OM, which also contributes to *Pseudomonas*' significant antibiotic resistance, is augmented by the presence of the outer membrane protein H (OprH). OprH directly interacts with lipopolysaccharides (LPS) that constitute the outer leaflet of the OM and thus contributes to the structural stability of the OM. In this study, we used solution NMR spectroscopy to characterize the interactions between LPS and OprH in molecular detail. NMR chemical shift perturbations observed upon the addition of LPS to OprH in DHPC micelles indicate that this interaction is predominantly electrostatic and localized to the extracellular loops 2 and 3 and a number of highly conserved basic residues near the extracellular barrel rim of OprH. Single-site mutations of these residues were not enough to completely abolish binding, but OprH with cumulative mutations of Lys70, Arg72, and Lys103 no longer binds LPS. The dissociation constant (~200 μM) measured by NMR is sufficient to efficiently bind LPS to OprH in the OM. This work highlights that solution NMR is suitable to study specific interactions of lipids with integral membrane proteins and provides a detailed molecular model for the interaction of LPS with OprH; i.e., an interaction that contributes to the integrity of the OM of *P. aeruginosa* under low divalent cation and antibiotic stress conditions. These methods should thus be useful for screening antibiotics that might disrupt OprH–LPS interactions and thereby increase the permeability of the OM of *P. aeruginosa*.

Graphical abstract

*Corresponding Author: lkt2e@virginia.edu. Phone: 434-982-3578.

The authors declare no competing financial interest.

Supporting Information

The Supporting Information is available free of charge on the ACS Publications website at DOI: 10.1021/acs.bio-chem.6b00630.

Four supplemental figures (PDF)

Author Manuscript Author Manuscript Author Manuscript Author Manuscript

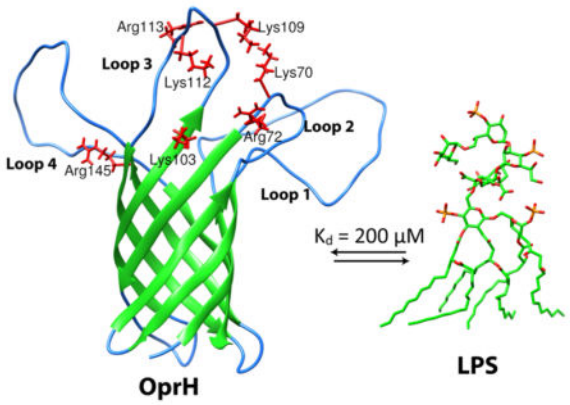

Pseudomonas aeruginosa is an opportunistic human pathogen and the most common cause of lung infections in cystic fibrosis patients.[1,2] *P. aeruginosa* is also responsible for high numbers of infections in hospital environments, including urinary tract, wound, and skin infections.[3,4] Compared with other pathogens, *P. aeruginosa* infections are very challenging to treat as this bacterium displays high intrinsic resistance to a wide range of antibiotics, including fluoroquinolones, aminoglycosides, and β-lactams. This is mainly caused by the high stability and low permeability of its outer membrane (OM), which is estimated to be 12–100 times less permeable than that of *Escherichia coli*, as well as the ability of *P. aeruginosa* to form resistant biofilms.[5,6] Lipopolysaccharides (LPS), which make up the outer leaflet of the OM, contribute a great deal to the high stability of *P. aeruginosa*'s OM. LPS produced by *P. aeruginosa* is a main factor in the virulence as well as innate and acquired host responses to infection.[7] LPS has a complex structure (Figure 1C). Its hydrophobic portion is lipid A, which by itself can elicit cytotoxicity. Attached to lipid A is a hydrophilic core polysaccharide chain, followed by the hydrophilic O-antigenic polysaccharide chain.[8] Removal of divalent cations from LPS by chelating agents and the binding of polycationic antibiotics such as polymyxins and aminoglycosides to LPS may lead to a destabilization and rupture of the OM.[9]

OprH is a 21-kDa protein integral to the OM of *P. aeruginosa*. OprH is genetically linked to the PhoP-PhoQ two-component regulatory system that is up-regulated in response to Mg^{2+}-limited growth conditions.[6,10] The PhoP-PhoQ system is also involved in virulence and in resistance to cationic antimicrobial peptides and polymyxin.[10] OprH is further up-regulated in bacteria that adhere to human bronchial epithelial cells 5000-fold compared to nonadherent bacterial cells.[11] This up-regulation occurs even when the culture medium contains millimolar concentrations of Mg^{2+} that would normally suppress transcription of the *oprH-phoP-phoQ* operon.[12] OprH might be a promising alternative target for antimicrobial treatments, as there has been a growing number of *P. aeruginosa* strains that are able to chemically modify their lipid A structure to gain resistance to last resort antibiotics like polymyxins.[13–15]

Solution NMR in 1,2-dihexanoyl-*sn*-glycero-3-phosphocholine (DHPC) micelles was used to determine the eight-stranded β-barrel structure of OprH, which also features four extracellular loops of unequal size (Figure 1A,B). NMR relaxation experiments revealed that

Author Manuscript Author Manuscript Author Manuscript Author Manuscript

the extracellular loops are unstructured and highly dynamic on the picosecond to nanosecond time-scale.[16] As mentioned, OprH is up-regulated and overexpressed so that it becomes a major component of the OM when *P. aeruginosa* is grown under limiting concentrations of divalent cations. Therefore, OprH is believed to act as a surrogate for Mg^{2+} and Ca^{2+} by cross-linking LPS, thereby tightening the OM during divalent cation defficiency.[10] The direct interaction of LPS with OprH was demonstrated using several *in vitro* and *in vivo* techniques, including NMR chemical shift perturbation, trypsin protection, and pull-down experiments.

On the basis of NMR chemical shift perturbations observed upon the addition of LPS to OprH in lipid micelles, it was concluded that the interaction is predominantly electrostatic and localized to charged regions near the extracellular rim of the barrel and loops 2 and 3 of OprH.[16] To characterize the binding site of LPS on OprH in more detail, we conducted a more comprehensive NMR study measuring chemical shift perturbations of backbone and side chain resonances upon the addition of LPS to OprH. We also removed several charged residues individually and in combination to test their effects on LPS binding. Combining our NMR results with binding studies using an enzyme-linked immunosorbent assay (ELISA) allowed us to present a more definitive molecular model for the interactions between LPS and OprH and offer new insight into protein–lipid interactions that may contribute to the antibiotic resistance during *P. aeruginosa* infections.

EXPERIMENTAL METHODS

Expression, Purification, and Refolding of OprH and OprG

OprH from *P. aeruginosa* strain PAO1 and all OprH mutants were expressed in BL21 (DE3) *E. coli* cells as described in refs 16 and 17. All OprH constructs used were without the N-terminal signal sequence (residues 1–22 were replaced with Met-1 so that Ala-23 becomes Ala-2 in our numbering system) and either with a C-terminal His_6-tag or Strep-tag II (SAWSHPQFEK). All proteins expressed into inclusion bodies in high yields.

^{2}H-,^{13}C-,^{15}N-labeled OprH with loops 1 and 4 deleted (OprHΔL1ΔL4) was used for the sequential assignment of the backbone, and ^{13}C-,^{15}N-labeled OprHΔL1ΔL4 was utilized for the assignment of side chains. For the preparation of [U-^{2}H,^{15}N]; Ileδ1-[$^{13}CH_3$]; Leu,Val-[$^{13}CH_3$,$^{12}CD_3$]-labeled samples, OprHΔL1ΔL4 cells were first grown overnight at 37 °C in 20 mL of unlabeled minimal media and then centrifuged at 5000 rpm for 10 min, washed with 5 mL of [U-^{2}H,^{15}N] minimal medium, centrifuged again, resuspended in 1 L of [U–^{2}H,^{15}N] minimal medium, and grown at 37 °C. When the OD_{600} reached 0.4, 60 mg of 2-keto-3-*d*2–4-^{13}C-butyrate and 100 mg of 2-keto-3-methyl-*d*3–3-*d*1–4-^{13}C-butyrate (Cambridge Isotope Laboratories) were added.[18] After 1 h the temperature was lowered to 25 °C, and protein overexpression was induced with 1 mM isopropyl-β-D-thiogalactopyranoside for ~16 h.

His_6-tagged proteins were purified from inclusion bodies and refolded following the published protocol.[17,19] Protein samples with a Strep-tag II used for NMR studies were solubilized from inclusion bodies in denaturation buffer (8 M urea, 10 mM MES pH 6.0, 0.1 mM EDTA) and loaded onto a hiTrap CM sepharose FF column (GE Healthcare Life

Author Manuscript Author Manuscript Author Manuscript Author Manuscript

Sciences). Proteins were eluted with a 0–250 mM NaCl gradient in denaturation buffer, concentrated to ~1 mL, and subsequently refolded. We also tried to use Strep-Tactin sepharose (iba) in our purification protocol, but we obtained only little to no protein binding to this resin. The final NMR samples were concentrated to 0.2–0.5 mM OprH in 25 mM $NaPO_4$ at pH 6.0, 50 mM KCl, 0.05% NaN_3, 5 mM EDTA, ~150 mM DHPC, and 5% D_2O.

Proteins with a Strep-tag II for ELISA were refolded immediately after solubilizing in inclusion bodies and then purified by gel-filtration on a Superdex 200 column (GE Healthcare Life Sciences) equilibrated with 20 mM HEPES pH 7.3, 150 mM NaCl, 1 mM EDTA, 0.1% DPC. Proteins at concentrations of ~0.5 mg/mL with good purity were obtained using this procedure, which effectively removed all free arginine used in the refolding buffer.[16] The proteins were quantitatively refolded as seen from the shift of their apparent molecular masses on SDS-PAGE gels.

OprG from *P. aeruginosa* strain PAO1 was expressed in BL21 (DE3) *E. coli* cells as described in refs 17 and 19. The OprG construct used was without the N-terminal signal sequence (residues 1–26 were replaced with Met1 so that His27 becomes His2 in our numbering system) and with a C-terminal Strep-tag II (SAWSHPQFEK). OprG-Strep-Tag II was purified the same way as OprH-Strep-Tag II for ELISA. SDS-PAGE gels showed pure and quantitatively refolded proteins.

Site-Directed Mutagenesis

The OprHΔL1ΔL4 mutant with loops 1 and 4 partially deleted was constructed by removing residues 17–38 and 150–167. Primers were designed to mutate positively charged residues 70, 72, 103, 113, and 145 to glutamines and to generate the double mutant R72Q/K103Q and the triple mutant K70Q/R72Q/K103Q. The Stratagene QuikChange site-directed mutagenesis kit was used to make all mutations starting with wild-type OprH.

Mass Spectroscopy

Samples of deep rough (Rd2) LPS from *E. coli* strain F583 (Sigma, #L6893) were prepared and analyzed by matrix-assisted laser desorption ionization-time-of-flight (MALDI-TOF) mass spectrometery as described in ref 20. A small amount of the LPS was solubilized in a mixture of methanol/water (1:1) containing 5 mM EDTA and dissolved by brief ultrasonication. A few microliters of the obtained mixture were then desalted on a small piece of Parafilm with some grains of cation-exchange beads (BT AG 50W-X8, Bio-Rad), previously converted into the ammonium form. A total of 0.3 μL of this sample solution was deposited, together with the same volume of 20 mM dibasic ammonium citrate, in a thin layer of homogeneous matrix film obtained from a solution, the components of which were 2,4,6-trihydroxyacetophenone (THAP), 200 mg/mL in methanol, and 15 mg/mL nitro-cellulose (Trans-blot membrane, BioRad) in acetone/propan-2-ol (1:1 v/v), mixed in a 4:1 v/v ratio.

Visualization of LPS on SDS-PAGE Gels by Zinc-Imidazole Staining

Rd2 LPS *E. coli* F583 was visualized on SDS-PAGE gels using zinc-imidazole staining, as described in ref 21. Briefly, after electrophoresis, the gel was incubated in 400 mL of boiling

Author Manuscript Author Manuscript Author Manuscript Author Manuscript

water (3 times for 15 min) to remove electrophoresis reagents. The water was removed, and the gel was incubated in 10 mM zinc sulfate for 15 min. To develop the image, the gel was soaked with agitation in 0.2 M imidazole for 1–3 min until a homogeneous white background developed on the gel surface except in the zones of the LPS bands, which remained transparent. After sufficient image contrast was attained, the gel was rinsed three times with 50–100 mL of distilled water to remove excess reagent. The appearance of the negative staining pattern was observed by placing the gel over any dark surface.

NMR Spectroscopy

All NMR experiments were recorded at 45 °C on a Bruker Avance III 800 spectrometer equipped with a triple-resonance cryoprobe. All double- and triple-resonance experiments were performed using the Bruker Topspin version 2.1.6 software suite. Sequential backbone assignments of OprHΔL1ΔL4 were obtained by recording TROSY versions of HNCA, HNCB, and HNCO experiments. Assignments of the $^{1}H–^{13}C$ HMQC spectrum of [U-^{2}H,^{15}N]; Ileδ1-[$^{13}CH_3$]; Leu,Val-[$^{13}CH_3$,$^{12}CD_3$] OprHΔL1ΔL4 were obtained by first collecting and assigning H(CCO)NH-TOCSY and (H)C(CO)NH-TOCSY spectra. All triple-resonance experiments were recorded in a nonuniformly sampled manner[22] using Poisson-gap sampling schedules[23] and reconstructed using the iterative soft threshold method.[24] All NMR data were processed with NMRPipe and analyzed with Sparky software.[25]

Enzyme-Linked Immunosorbant Assay

ELISAs were performed following the protocol of ref 26, with several modifications. Nunc MaxiSorp ELISA plates (BioLegend) were coated by incubating 100 μL of 30 μg/mL LPS from *E. coli* F583 (Sigma) in 0.1 M Na_2CO_3, 20 mM EDTA, pH 9.6, overnight at 37 °C. The LPS solution was flicked out, and the plates were rinsed three times with water. Excess binding sites were blocked with 100 μL/well of 10 mg/mL BSA in 50 mM HEPES, 0.15 M NaCl, 1 mM EDTA, pH 7.4 for 30 min at 37 °C. Refolded protein samples with the C-terminal Strep-tag II were added in a total volume of 100 μL/well diluted in 50 mM HEPES, 0.15 M NaCl, 1 mM EDTA, 1 mg/mL BSA, 0.05% Tween 20 (Sigma) (buffer A). Binding was allowed to occur for 3 h at 37 °C. The plate was then rinsed three times with 200 μL/well of buffer A. Anti-Strep II StrepMAB-Classic antibody (iba), 100 μL/well diluted 5000× in buffer A was added to each well and incubated for 1 h at room temperature with agitation. Subsequently the plate was rinsed three times with 200 μL/well of buffer A. Antimouse IgG peroxidase conjugate antibody (Sigma), 100 μL/well diluted 5000× in buffer A was added and incubated in the wells for 1 h at room temperature with agitation followed by three washes of 200 μL/well buffer A. The peroxidase substrate 3,3′,5,5′ tetramethylbenzidine (Sigma) 100 μL/well was added undiluted to each well and incubated for 15 min at room temperature with agitation. The reaction was stopped by addition of 0.5 M sulfuric acid and the absorbance was read at 450 nm on a SpectraMax M5 (Molecular Devices) plate reader. The mean absorbances and standard errors were calculated from six replicates of each well.

Lysine Methylation

Reductive methylation was performed following the protocols of refs 27 and 28 with the following modifications. Briefly, 20 μL of a 1 M borane–ammonia complex ($NH_3–BH_3$) and 40 μL of 1 M formaldehyde were added to 1 mL of 0.5 M purified and unfolded OprH in 50

Author Manuscript Author Manuscript Author Manuscript Author Manuscript

mM $NaPO_4$ at pH 8.0, 300 mM NaCl, 8 M urea, 250 mM imidazole, and the reaction was incubated for 2 h with stirring at 25 °C. The addition of the borane–ammonia complex and formaldehyde was repeated, and the mixture was incubated for another 2 h. After the addition of another 10 μL of 1 M borane–ammonia complex, the reaction mixture was incubated at 25 °C with stirring overnight. The reaction was stopped by adding glycine to 200 mM, and undesired reaction products as well as excess reagents were removed by purification on PD-10 desalting column (GE Healthcare Life Sciences). The resulting lysine-methylated OprH was refolded using the same procedure as unmodified, wild-type OprH. After refolding, the labeling was confirmed by MALDI analysis.

Determination of LPS-OprH Dissociation Constants by NMR

The dissociation constant for the binding of LPS to OprH was determined by monitoring the change in chemical shifts of ^{15}N–^{1}H-TROSY cross-peaks as a function of the LPS concentration as described in ref 29. 0.1–0.15 mM ^{15}N-labeled OprH, OprH-R72Q or OprHΔL1ΔL4 in 25 mM $NaPO_4$ at pH 6.0, 50 mM KCl, 0.05% NaN_3, 5 mM EDTA, ~150 mM DHPC and 5% D_2O was titrated with seven or eight additions of Rd2 LPS from *E. coli* F583 so that the final concentration of LPS was 1.7–4.0 mM. ^{15}N TROSY spectra were recorded in triplicate with each successive addition. The difference in chemical shift of an atom with no LPS present and that in the presence of LPS ($\Delta\delta_{obs}$) was plotted against the total amount of LPS added (LPS_{tot}) and fitted with the equation:

$$\Delta\delta_{\mathrm{obs}}/\Delta\delta_{\mathrm{max}}=\{(K_{\mathrm{d}}+\mathrm{LPS}_{\mathrm{tot}}+\mathrm{OprH}_{\mathrm{tot}})-[(K_{\mathrm{d}}+\mathrm{LPS}_{\mathrm{tot}}+\mathrm{OprH}_{\mathrm{tot}})^2-4\cdot\mathrm{LPS}_{\mathrm{tot}}\cdot\mathrm{OprH}_{\mathrm{tot}}]^{1/2}\}/(2\cdot\mathrm{OprH}_{\mathrm{tot}}) \quad (1)$$

where K_d is the dissociation constant, $OprH_{tot}$ is the total amount of OprH present in solution, and $\Delta\delta_{max}$ is the maximum chemical shift difference seen for the given residue of the protein saturated with LPS.

RESULTS

Characterization of Different Species of LPS Used for Assessing Their Interactions with OprH

Different species and strains of Gram-negative bacteria produce different varieties of LPS. In order to analyze interactions of LPS with OprH by NMR, we tested multiple products of LPS for their suitability in interaction studies by solution NMR. Commercially available smooth LPS from *P. aeruginosa* (Sigma, #L8643, #L9143, #L7018) has highly variable chemical compositions and contents of impurities. We found that when used at high concentrations needed for NMR, these sources of LPS produce viscous solutions that deteriorate the quality of NMR spectra. Deep rough (Rd2) LPS from *E. coli* strain F583 (Sigma, #L6893) (Figure 1C) behaved better and was used in studies that required a high excess of LPS over protein concentrations, most notably the NMR titration studies. To verify the molecular mass of Rd2 LPS from *E. coli* strain F583 we performed MALDI-MS analysis

Author Manuscript Author Manuscript Author Manuscript Author Manuscript

(Figure S1A) and SDS-PAGE electrophoresis followed by staining with zinc and imidazole salts[21] (Figure S1B). Since Rd2 LPS is prone to aggregate, a clear band at ~2.7 kDa was observed on SDS-PAGE only when the protein was loaded at lower concentration. The molecular mass of 2.7 kDa is consistent with the MALDI-MS result. Best results for NMR assignments and chemical shifts of OprH were obtained with Kdo2-lipid A (Avanti Polar Lipids, #699500P), which lacks the outer core polysaccharide rings. The chemical structure (Figure 1C,D) and molecular mass (2306 Da) of this product is better defined and more uniform compared to other commercially available LPS samples. We confirmed that the ^{15}N-TROSY spectrum of OprH with Kdo2-lipid A was similar but of better quality than the previously reported spectrum of OprH in the presence of *P. aeruginosa* smooth LPS.[16] The solubility of Kdo2-lipid A is lower than that of Rd2 LPS but is still sufficient for most of the NMR work reported in this study.

NMR Chemical Shift Perturbation of ΔL1,ΔL4 Mutant of OprH by Kdo2-LipidA

We previously showed that the interaction of OprH with LPS is mainly mediated through loops 2 and 3.[16] Therefore, and to simplify assignments, we used an OprH construct with loops 1 and 4 deleted (OprHΔL1ΔL4) in this work. This protein yielded a ^{15}N–^{1}H -TROSY spectrum with significantly less overlap in the region from 7.8 to 8.6 ^{1}H ppm compared to wild-type OprH, which permitted a de novo assignment of this construct (Figure 2A). To determine which specific residues of OprHΔL1ΔL4 interact with LPS, Kdo2-lipid A was added to 0.2 mM ^{2}H-,^{13}C-,^{15}N-labeled OprHΔL1ΔL4 in DHPC micelles to a final ratio of 10:1 Kdo2-lipid A to OprHΔL1ΔL4. The overlay of this spectrum onto the spectrum of OprHΔL1ΔL4 in DHPC revealed many changes of backbone chemical shifts (Figure 2A,B). Addition of Rd2 LPS from *E. coli* to OprHΔL1ΔL4 (Figure S2A,B) resulted in similar chemical shifts as observed with Kdo2-lipid A. However, Rd2 LPS also caused more significant broadening of many resonance lines compared to Kdo2-lipid A. The ^{15}N–^{1}H TROSY spectra of OprHΔL1ΔL4 in DHPC and in DHPC/Kdo2-lipid A micelles were assigned, by recording TROSY versions of HNCA, HNCB, and HNCO experiments. The resulting chemical shift perturbations are very similar to those observed with wild-type OprH (data not shown). The most significant chemical shift changes (>0.05 ppm) are found at the base of loop 1 (residues G11, E12, T13, T39, G40), in loop 2 (residues E60-L71 and N75), at the base of loop 3 (residues V102 and K103 and residues K112, R113, S115, and V117), and in β-strand 8 (residues Q170-G174 and F179-E181). Addition of 2 mM 1-myristoyl-2-hydroxy-*sn*-glycero-3-phospho-(1′-*rac*-glycerol) (LMPG, Avanti), which is a negatively charged lipid with the same acyl chain length as Kdo2-lipid A, to OprHΔL1ΔL4 resulted in significant chemical shift changes in common with Kdo2-lipidA in β-strands 1,7, and 8, but not in loops 2 and 3 or the base of loop 1. This indicates that the perturbations in the positively charged loops of OprHΔL1ΔL4 are specific to the addition of Kdo2-lipid A and are not the generic result of its negative charge or hydrophobic acyl chains. Addition of $MgCl_2$ to the OprHΔL1ΔL4:Kdo2-lipid A resulted in chemical shift changes of many loop residues back to the chemical shifts observed with the OprHΔL1ΔL4 sample without Kdo2-lipid A.

To obtain more insight into interactions between the hydrophobic amino acid side chains of OprHΔL1ΔL4 and the acyl chains of lipid A, Kdo2-lipid A was added to a sample of 0.2

Author Manuscript Author Manuscript Author Manuscript Author Manuscript

mM [U-^{2}H,^{15}N]; Ileδ1-[^{13}CH$_3$]; Leu,Val-[^{13}CH$_3$,^{12}CD$_3$]-labeled OprHΔL1ΔL4 in DHPC micelles to a final ratio of 10:1 Kdo2-lipid A to protein, and the ^{1}H–^{13}C HMQC spectrum of this complex was collected (Figure 3A,B). The resonances of the methyl groups of these side chains can be assigned by correlation to the backbone amide resonances of the following residues using a combination of H(CCO)NH-TOCSY and (H)C(CO)NH-TOCSY spectra. This strategy allowed us to unambiguously assign the methyl groups of all isoleucines, all valines, and 12 of the 15 leucines. The overlay of the ^{1}H–^{13}C HMQC spectrum recorded at a 10:1 Kdo2-lipid A/OprH ratio onto the spectrum of OprHΔL1ΔL4 in DHPC only revealed multiple side-chain chemical shift perturbations in β-strand 1, the base of loop 3 and β-strand 8. Only one loop residue, Ile62 of loop 2, was observed to show a moderate chemical shift perturbation. In general, the resulting pattern of side chain chemical shift perturbations closely follows the one obtained for the backbone resonances that were observed in OprHΔL1ΔL4 ^{15}N–^{1}H TROSY spectrum upon addition of Kdo2-lipid A. We also collected the ^{1}H–^{13}C HMQC spectrum of [U–^{2}H,^{15}N]; Ileδ1-[^{13}CH$_3$]; Leu,Val-[^{13}CH$_3$,^{12}CD$_3$]-labeled OprHΔL1ΔL4 in the presence of LMPG instead of Kdo2-lipid A. This spectrum appeared to be identical to the spectrum of OprHΔL1ΔL4 in the absence of LMPG, confirming that the observed Kdo–lipid A interactions are specific to this lipid (data not shown).

Since Kdo2-lipid A contains two phosphate groups which impart a net negative charge on the molecule, it is reasonable to assume that these lipid phosphates interact electrostatically with the side chains of basic amino acid residues. A comparison of the amino acid sequences of OprH homologues from different *Pseudomonads* reveals a high degree of similarity, with several conserved regions, especially in the β-strands (Figure S3). Of the seven basic residues that are localized at the extracellular upper rim of the β-barrel, five, namely, K70, R72, K103, R113, and R145, are absolutely conserved. To test the hypothesis that LPS interacts with basic residues at the barrel rim or in loops 2 and 3, we collected H(C) (CC)-TOCSY-(CO)-[^{15}N,^{1}H]-TROSY spectra of a ^{13}C-,^{15}N-labeled OprHΔL1ΔL4 sample with and without 10-fold excess of Kdo2-lipid A (Figure 4). A subset of side chains could be observed in this experiment, including the side chains of K109, K112 and R113, which all reside in loop 3 (Figure 1). The side chains of the remaining basic residues could not be detected due to line-broadening. The side chain chemical shifts of K109 and K112 were not changed upon the addition of Kdo2-lipid A, but the ^{15}N chemical shift of R113 changed slightly (Figure 4A,C). Adding Kdo2-lipid A resulted in further line-broadening and a decrease in peak intensity of these residues (Figure 4A,B). While the side chain cross peaks of K109 and K112 experienced an intensity decrease on the order of 50%, the intensities of the side chain resonances of R113 decreased about 75% in the presence of Kdo2-lipidA. Interestingly, the more strongly interacting rim residue R113 belongs to the absolutely conserved basic residues, whereas the more weakly interacting residues K109 and K112 are localized in loop 3 and do not appear to be conserved in OprH homologues of *Pseudomonads* (Figure S3).

Measurement of OprH–LPS Interactions by ELISA

To measure the binding of OprH to LPS we adapted a solid-phase enzyme-linked immunosorbent assay by immobilizing Rd2 LPS on a microtiter plate and measuring the

Author Manuscript Author Manuscript Author Manuscript Author Manuscript

binding of refolded OprH in DHPC lipid micelles. Since we are not aware of the availability of an anti-OprH antibody, we first attempted to use an anti-PentaHis antibody (Qiagen) on His-tagged OprH. However, we observed a large amount of unspecific binding with this antibody and therefore decided to replace the C-terminal 6xHis-tag with a Strep-tag II. High quality antibodies against this tag are commercially available. In Figure 5A we show the concentration-dependent binding of OprH-Strep-tag II to the LPS-coated microtiter plate, which saturates at around 10 μg/mL of OprH. We next used this assay to compare the influence of various conditions and mutations on the binding affinity of OprH to Rd2 LPS (Figure 5B). We used 1 μg/mL protein concentrations in these assays because the binding response is most sensitive in this low concentration regime.

When any of the assay components were omitted, a 450 nm absorbance of less than 0.06 developed in the microtiter well (Figure 5B, first lane) compared to more than 0.16 absorbance units for 1 μg/mL wild-type OprH in the presence of all assay components (Figure 5B, second lane). Heat-denatured OprH (90 °C, 30 min) yielded 0.07 units when it was used in place of refolded OprH. Using another outer membrane protein (OMP) from *P. aeruginosa* with a similar β-barrel structure, OprG, which has no known LPS binding activity, resulted in no detectable signal at both 1 and 10 μg/mL protein concentrations. Coating the wells with different lipids such as POPC gave little to no signal. When polymyxin B was added after OprH had bound to LPS in the well, the signal was reduced by 40%, indicating that polymxyxin B is able to partially disrupt the OprH–LPS interaction or remove the OprH-LPS complex from the microtiter plate. Interestingly, the global methylation of the ε-NH_3 groups in all lysines of OprH resulted in a 30% weaker binding compared to unmodified OprH. This suggests that not only the charge but perhaps also the ability of lysines to form hydrogen bonds could be important for binding to LPS.

To analyze the effect of individual conserved basic residues on the ability of OprH to bind LPS, we individually mutated K70, R72, K103, R113, and R145 to glutamines. All of these single mutants showed weaker binding than wild-type (Figure 5B). The most significant decrease was observed with R72Q (32% less binding), and the least significant decrease occurred with R145Q (15% less binding). Although perhaps statistically significant only as a trend, the contributions of the individual residues to LPS binding decrease in the order R72 > K103 ≈ K70 > R113 > R145. This result is consistent with the previous result that the removal of any single loop is not sufficient to abolish the binding of LPS to OprH.[16] However, mutation of two positive charges, namely, R72Q on loop 2 and K103Q on loop 3, reduced binding more than each single mutant, and the triple mutant K70Q/R72Q/K103Q reduced LPS binding close to the level of boiled OprH.

Mutant Loop Interactions and Determination of Dissociation Constants of LPS–OprH Binding by NMR

To determine if the previously described structural effects that LPS binding has on OprH is mitigated in these mutants with decreased binding, we expressed ^{15}N-labeled OprH-R72Q, OprH-R72Q/K103Q, and OprH-K70Q/R72Q/K103Q and collected their respective ^{15}N–^{1}H-TROSY spectra with and without Kdo2-lipid A at 10:1 lipid/protein ratios (Figure S4). The chemical shifts of OprH-R72Q were less perturbed in the loop 2 region upon addition of

Author Manuscript Author Manuscript Author Manuscript Author Manuscript

Kdo2-lipid A than in the wild-type protein. In the case of the double mutant OprH-R72Q/K103Q the resonances of most loop residues did not shift at all. However, OprH-K70Q/R72Q/K103Q showed a significantly different NMR spectrum with the loop resonances in the 7.6–8.4 ^{1}H ppm region significantly stronger compared to wild-type suggesting that removing all three positive charges might alter the folding and dynamics of the loops or introduces some other global changes on the protein.

To more quantitatively measure the binding of LPS to OprH, we titrated Rd2 LPS to wild-type ^{2}H,^{15}N-labeled OprH and OprHΔL1ΔL4 samples. The dissociation constant for the binding of LPS to OprH was estimated using the chemical shifts derived from the ^{15}N–^{1}H TROSY cross-peaks of several loop 3 residues and eq 1. The K_d was found to be approximately 0.2 mM for wild-type OprH (Figure 6A) and OprHΔL1ΔL4 (Figure 6B). The R72Q mutant OprH, which showed the weakest binding of the all single mutants that were tested by ELISA, exhibited a K_d value of approximately 0.6 mM, i.e., about a 3-fold weaker binding than wild-type OprH (Figure 6C). These binding curves were measured using $^{1}H_N$ chemical shifts of the resonances of only loop 3 cross-peaks that showed significant changes upon addition of LPS and that had no overlap with other resonances. We were unable to use resonances of loop 2 for an independent K_d determination because the resonance lines of these cross-peaks were more overlapped and more broadened upon addition of LPS than those of loop 3.

DISCUSSION

Lipid interactions with integral membrane proteins have been studied for as long as the fluid mosaic model of biological membranes exists. While early studies debated if an annulus of distinct boundary lipids exists around integral membrane proteins,[30] research has focused in more recent years on specific lipid–protein interactions. There are now over 100 crystal structures available of membrane proteins that contain density that has been interpreted as specifically bound lipid.[31] Likewise, mass spectrometry has identified many integral membrane proteins that are ionized and desorbed from their preparation substrate with certain lipids bound.[32] But, are these lipids also specifically bound to membrane proteins in a membrane environment? Or, are they cocrystallized simply to maintain the stability of the membrane protein and are they just “hanging on” when the membrane protein “flies” through vacuum in the mass spectrometer? The answers to these questions are generally not known, and it is possible, perhaps even likely, that no general answer exists. Some pairs of lipids and proteins may interact specifically when probed in membrane or micellar environments, whereas others may be prompted by the special circumstances of sample handling in crystallography and mass spectrometry. Solution NMR has also been employed in relatively rare cases to investigate specific lipid interactions with integral membrane proteins in lipid micelles and bicelles. A prominent example is a study on the interaction of cholesterol with the amyloid precursor protein $APP_{672–770}$.[33]

In this work, we explored further the possibility to study specific lipid–protein interactions by NMR in lipid micelles in solution. The previously identified interaction between the OM lipid LPS and the *Pseudomonas aeruginosa* OMP OprH[16] was chosen for this purpose. We found that the acidic LPS binds to basic residues in loops 2 and 3 and at the extracellular rim

Author Manuscript Author Manuscript Author Manuscript Author Manuscript

of the β-barrel of OprH. This electrostatic interaction is reminiscent of the interaction of the *E. coli* OMP FhuA with LPS,[34] which to the best of our knowledge is the only other membrane protein, for which detailed molecular interactions with LPS have been reported. The structure of FhuA, which is responsible for ferric hydroxamate uptake in *E. coli*, was solved in complex with LPS. Analysis of this structure revealed that the contacts between the protein and LPS are mainly through the phosphate residues of lipid A and Kdo I and II sugar moieties, which constitutes a region of LPS that is highly conserved in all Gram-negative bacteria. As with OprH, strong electrostatic interactions were observed between basic, positively charged amino acids of FhuA and the negatively charged phosphates on the lipid A and inner core carbohydrate moieties of LPS. The LPS binding area covered a significant fraction of the surface of FhuA that included four strands and two extracellular loops. Our analysis of the binding interface between OprH and LPS reveals similar molecular interactions. The width of the OprH LPS binding site is similar to the width of the lipid A molecule (Figure 1), and therefore it seems reasonable to assume that the LPS binding stoichiometry is 1:1, as is the case for LPS binding to FhuA[34] and polymyxin B.[35]

By analyzing NMR chemical shift perturbations of OprH backbone and side chain resonances upon the addition of LPS, we found that the specific interaction is localized to the extracellular loops 2 and 3 and the base of loop 1. The resonances of numerous residues in these regions were shifted by LPS, but not by a non-LPS lipid of similar charge and hydrophobic acyl chain length. This suggests that the basic residues of loops 2 and 3 form hydrogen bonds with the negatively charged phosphates of the inner core region of LPS, and as a result the glucosamine backbone of lipid A is placed in close proximity to the base of extracellular loop 1. Smaller shifts in the region of β-strands 1, 7, and 8 were not only observed with LPS, but also with LMPG. Therefore, these interactions are most likely due to general hydrophobic interactions with the long acyl chains of these lipids that, when present, displace the short chain lipid DHPC.

The importance of several conserved basic residues was further supported by our ELISA binding analysis, which indicates that single mutations of arginines and lysines in loops 2 and 3 significantly decrease the binding affinity, while double and triple mutations lead to a loss of LPS binding. Interestingly, ε-NH_3 methylation of the lysines of OprH also significantly decreased LPS binding, which suggests that the capability of the primary amine of lysine to form hydrogen bonds is also important and not just its charge, which is preserved in the quaternary amine of the methylated species. Alternatively, the bulkiness of the methylated side chain may be detrimental to LPS binding.

The binding of LPS to OprH with $K_d \approx 200\ \mu M$ appears to be relatively weak when simply considered as a binary interaction in solution. However, the binding of LPS to its binding site on OprH is actually highly efficient if one considers the very high density of LPS in the bacterial OM. Given a local “concentration” of LPS close to 1 M, a K_d of a few hundred μM is by far suficient to occupy each binding site with a LPS molecule. Although Mg^{2+} and Ca^{2+} bind to LPS with a K_d of approximately 10 μM,[36] OprH takes the place of divalent cations in binding LPS under low divalent cation conditions, as has been documented physiologically.[16] This effect should be enhanced in the membrane compared to micellar

Author Manuscript Author Manuscript Author Manuscript Author Manuscript

solutions because the local concentrations of lipids and proteins in the membrane are orders of magnitude higher than even high concentrations of divalent cations in solution.

In this work, we have mainly used Kdo2-lipid A and Rd2 LPS from *E. coli*, as they have inner core regions that are similar to the inner core regions of *P. aeruginosa* smooth LPS.[37] However, the smaller size of the *E. coli* species used in this study simplifies their use in solution NMR experiments. The most significant difference between *P. aeruginosa* LPS and *E. coli* LPS lies in their acyl chains. The most common acyl chain length is 14 carbons in the case of *E. coli* and 10–12 carbons in the case of *P. aeruginosa*. In addition, *E. coli* synthesizes mainly hexa-acetylated LPS, while laboratory adapted strains of *P. aeruginosa* produce ~75% penta-acetylated LPS and 25% hexa-acetylated LPS.[38,39] *P. aeruginosa* strains synthesizing hepta-acetylated lipid A, which contain an additional palmitoyl (16:0) chain linked to the primary 3-hydroxy-decanoic acid group, have also been isolated.[38,40] However, because of the heterogeneity in acyl chain composition of LPS that is produced by *P. aeruginosa,* it is unlikely that the acyl chains are a key part of the LPS–OprH interaction.

In conclusion, we have identified several key residues that are responsible for the binding of LPS to OprH. We have also established the dissociation constant for this interaction that likely contributes to antibiotic resistance during *P. aeruginosa* infections. Beyond the specific LPS–OprH interaction, this work also demonstrates the versatility of modern solution NMR, from establishing protein structure and investigating protein backbone and side chain dynamics to the identification of binding sites and dissociation constants of selectively binding membrane lipids that cannot be easily achieved by other analytical methods.

Supplementary Material

Refer to Web version on PubMed Central for supplementary material.

Acknowledgments

Funding

This work was supported by NIH Grant R01 GM51329.

We acknowledge the W. M. Keck Biomedical Mass Spectrometry Laboratory at the University of Virginia. We thank Dr. Jeff Ellena of the Biomolecular Magnetic Resonance Facility of the University of Virginia for many helpful suggestions.

References

1. Govan JR, Brown AR, Jones AM. Evolving epidemiology of Pseudomonas aeruginosa and the Burkholderia cepacia complex in cystic fibrosis lung infection. Future Microbiol. 2007; 2:153–164. [PubMed: 17661652]
2. Rajan S, Saiman L. Pulmonary infections in patients with cystic fibrosis. Semin Respir Infect. 2002; 17:47–56. [PubMed: 11891518]
3. Gellatly SL, Hancock RE. Pseudomonas aeruginosa: new insights into pathogenesis and host defenses. Pathog Dis. 2013; 67:159–173. [PubMed: 23620179]
4. Silby MW, Winstanley C, Godfrey SA, Levy SB, Jackson RW. Pseudomonas genomes: diverse and adaptable. FEMS Microbiol Rev. 2011; 35:652–680. [PubMed: 21361996]
5. Hancock RE. Resistance mechanisms in Pseudomonas aeruginosa and other nonfermentative gram-negative bacteria. Clin Infect Dis. 1998; 27(Suppl 1):S93–S99. [PubMed: 9710677]

Author Manuscript Author Manuscript Author Manuscript Author Manuscript

6. Nicas TI, Hancock RE. Pseudomonas aeruginosa outer membrane permeability: isolation of a porin protein F-deficient mutant. J Bacteriol. 1983; 153:281–285. [PubMed: 6294050]
7. Koebnik R, Locher KP, Van Gelder P. Structure and function of bacterial outer membrane proteins: barrels in a nutshell. Mol Microbiol. 2000; 37:239–253. [PubMed: 10931321]
8. Mayer H, Tharanathan RN, Weckesser J. Analysis of lipopolysaccharides of gram-negative bacteria. Methods Microbiol. 1985; 18:157–207.
9. Vaara M. Agents that increase the permeability of the outer membrane. Microbiol Rev. 1992; 56:395–411. [PubMed: 1406489]
10. Macfarlane EL, Kwasnicka A, Hancock RE. Role of Pseudomonas aeruginosa PhoP-phoQ in resistance to antimicrobial cationic peptides and aminoglycosides. Microbiology. 2000; 146:2543–2554. [PubMed: 11021929]
11. Gellatly SL, Needham B, Madera L, Trent MS, Hancock RE. The Pseudomonas aeruginosa PhoP-PhoQ two-component regulatory system is induced upon interaction with epithelial cells and controls cytotoxicity and inflammation. Infect Immun. 2012; 80:3122–3131. [PubMed: 22710876]
12. Macfarlane EL, Kwasnicka A, Ochs MM, Hancock RE. PhoP-PhoQ homologues in Pseudomonas aeruginosa regulate expression of the outer-membrane protein OprH and polymyxin B resistance. Mol Microbiol. 1999; 34:305–316. [PubMed: 10564474]
13. Miller AK, Brannon MK, Stevens L, Johansen HK, Selgrade SE, Miller SI, Hoiby N, Moskowitz SM. PhoQ mutations promote lipid A modification and polymyxin resistance of Pseudomonas aeruginosa found in colistin-treated cystic fibrosis patients. Antimicrob Agents Chemother. 2011; 55:5761–5769. [PubMed: 21968359]
14. Mueller P, Rudin DO, Tien HT, Wescott WC. Reconstitution of cell membrane structure in vitro and its transformation into an excitable system. Nature. 1962; 194:979–980. [PubMed: 14476933]
15. Muller C, Plesiat P, Jeannot K. A two-component regulatory system interconnects resistance to polymyxins, aminoglycosides, fluoroquinolones, and beta-lactams in Pseudomonas aeruginosa. Antimicrob Agents Chemother. 2011; 55:1211–1221. [PubMed: 21149619]
16. Edrington TC, Kintz E, Goldberg JB, Tamm LK. Structural basis for the interaction of lipopolysaccharide with outer membrane protein H (OprH) from Pseudomonas aeruginosa. J Biol Chem. 2011; 286:39211–39223. [PubMed: 21865172]
17. Kucharska I, Edrington TC, Liang B, Tamm LK. Optimizing nanodiscs and bicelles for solution NMR studies of two beta-barrel membrane proteins. J Biomol NMR. 2015; 61:261–274. [PubMed: 25869397]
18. Tugarinov V, Kanelis V, Kay LE. Isotope labeling strategies for the study of high-molecular-weight proteins by solution NMR spectroscopy. Nat Protoc. 2006; 1:749–754. [PubMed: 17406304]
19. Kucharska I, Seelheim P, Edrington T, Liang B, Tamm LK. OprG Harnesses the Dynamics of its Extracellular Loops to Transport Small Amino Acids across the Outer Membrane of Pseudomonas aeruginosa. Structure. 2015; 23:2234–2245. [PubMed: 26655471]
20. Sturiale L, Garozzo D, Silipo A, Lanzetta R, Parrilli M, Molinaro A. New conditions for matrix-assisted laser desorption/ionization mass spectrometry of native bacterial R-type lipopolysaccharides. Rapid Commun Mass Spectrom. 2005; 19:1829–1834. [PubMed: 15945032]
21. Hardy E, Pupo E, Castellanos-Serra L, Reyes J, Fernandez-Patron C. Sensitive reverse staining of bacterial lipopolysaccharides on polyacrylamide gels by using zinc and imidazole salts. Anal Biochem. 1997; 244:28–32. [PubMed: 9025903]
22. Hyberts SG, Arthanari H, Wagner G. Applications of non-uniform sampling and processing. Top Curr Chem. 2011; 316:125–148.
23. Hyberts SG, Milbradt AG, Wagner AB, Arthanari H, Wagner G. Application of iterative soft thresholding for fast reconstruction of NMR data non-uniformly sampled with multidimensional Poisson Gap scheduling. J Biomol NMR. 2012; 52:315–327. [PubMed: 22331404]
24. Hyberts SG, Takeuchi K, Wagner G. Poisson-gap sampling and forward maximum entropy reconstruction for enhancing the resolution and sensitivity of protein NMR data. J Am Chem Soc. 2010; 132:2145–2147. [PubMed: 20121194]
25. Goddard, TD., Kneller, DG. SPARKY 3. University of California; San Francisco:

Author Manuscript Author Manuscript Author Manuscript Author Manuscript

26. Tobias PS, Soldau K, Ulevitch RJ. Identification of a lipid A binding site in the acute phase reactant lipopolysaccharide binding protein. J Biol Chem. 1989; 264:10867–10871. [PubMed: 2471708]
27. Abraham SJ, Hoheisel S, Gaponenko V. Detection of protein-ligand interactions by NMR using reductive methylation of lysine residues. J Biomol NMR. 2008; 42:143–148. [PubMed: 18819009]
28. Means GE, Feeney RE. Reductive alkylation of amino groups in proteins. Biochemistry. 1968; 7:2192–2201. [PubMed: 5690712]
29. Fielding L. NMR methods for the determination of protein-ligand dissociation constants. Curr Top Med Chem. 2003; 3:39–53. [PubMed: 12577990]
30. Seelig, J., Seelig, A., Tamm, LK. Nuclear Magnetic Resonance and Lipid-Protein Interactions. Vol. 2. John R. Wiley & Sons; New York: 1982.
31. Yeagle PL. Non-covalent binding of membrane lipids to membrane proteins. Biochim Biophys Acta, Biomembr. 2014; 1838:1548–1559.
32. Laganowsky A, Reading E, Allison TM, Ulmschneider MB, Degiacomi MT, Baldwin AJ, Robinson CV. Membrane proteins bind lipids selectively to modulate their structure and function. Nature. 2014; 510:172–175. [PubMed: 24899312]
33. Barrett PJ, Song Y, Van Horn WD, Hustedt EJ, Schafer JM, Hadziselimovic A, Beel AJ, Sanders CR. The amyloid precursor protein has a flexible transmembrane domain and binds cholesterol. Science. 2012; 336:1168–1171. [PubMed: 22654059]
34. Ferguson AD, Welte W, Hofmann E, Lindner B, Holst O, Coulton JW, Diederichs K. A conserved structural motif for lipopolysaccharide recognition by procaryotic and eucaryotic proteins. Structure. 2000; 8:585–592. [PubMed: 10873859]
35. Srimal S, Surolia N, Balasubramanian S, Surolia A. Titration calorimetric studies to elucidate the specificity of the interactions of polymyxin B with lipopolysaccharides and lipid A. Biochem J. 1996; 315(Pt 2):679–686. [PubMed: 8615847]
36. Schindler M, Osborn MJ. Interaction of divalent cations and polymyxin B with lipopolysaccharide. Biochemistry. 1979; 18:4425–4430. [PubMed: 226126]
37. Kabanov DS, Prokhorenko IR. Structural analysis of lipopolysaccharides from Gram-negative bacteria. Biochemistry (Moscow). 2010; 75:383–404. [PubMed: 20618127]
38. Ernst RK, Hajjar AM, Tsai JH, Moskowitz SM, Wilson CB, Miller SI. Pseudomonas aeruginosa lipid A diversity and its recognition by Toll-like receptor 4. J Endotoxin Res. 2003; 9:395–400. [PubMed: 14733728]
39. Pier GB. Pseudomonas aeruginosa lipopolysaccharide: a major virulence factor, initiator of inflammation and target for effective immunity. Int J Med Microbiol. 2007; 297:277–295. [PubMed: 17466590]
40. Ernst RK, Yi EC, Guo L, Lim KB, Burns JL, Hackett M, Miller SI. Specific lipopolysaccharide found in cystic fibrosis airway Pseudomonas aeruginosa. Science. 1999; 286:1561–1565. [PubMed: 10567263]

Author Manuscript Author Manuscript Author Manuscript Author Manuscript

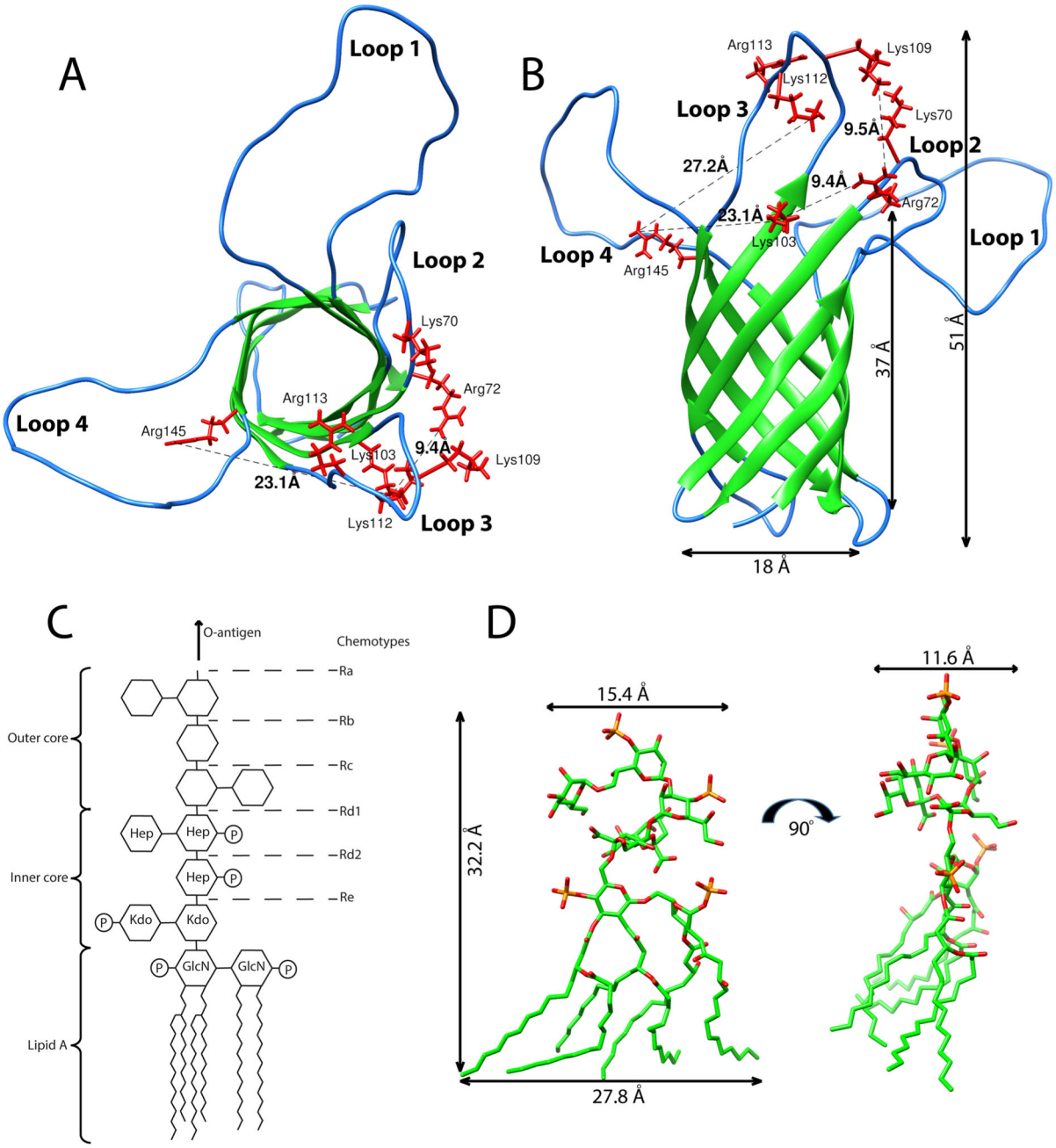

Figure 1.

Comparison of structures of OprH and LPS. (A) and (B) OprH from *P. aeruginosa* (PDB code: 2LHF). Charged side chains that might interact with LPS are highlighted in red and the distances between the distal residues are shown as black dashed lines. (C) Schematic chemical structure of *E. coli* LPS. LPS is composed of lipid A, inner and outer core oligosaccharides, and O-antigens. GlcN, D-glucosamine; Kdo, 3-deoxy-D-manno-octulsonic acid; Hep, L-glycero-D-mannoheptose; P, phosphate. (D) Dimension of Rd LPS based on the crystal structure of the TLR4/MD-2/Ra LPS complex (PDB code: 3FXI).

Author Manuscript
Author Manuscript
Author Manuscript
Author Manuscript

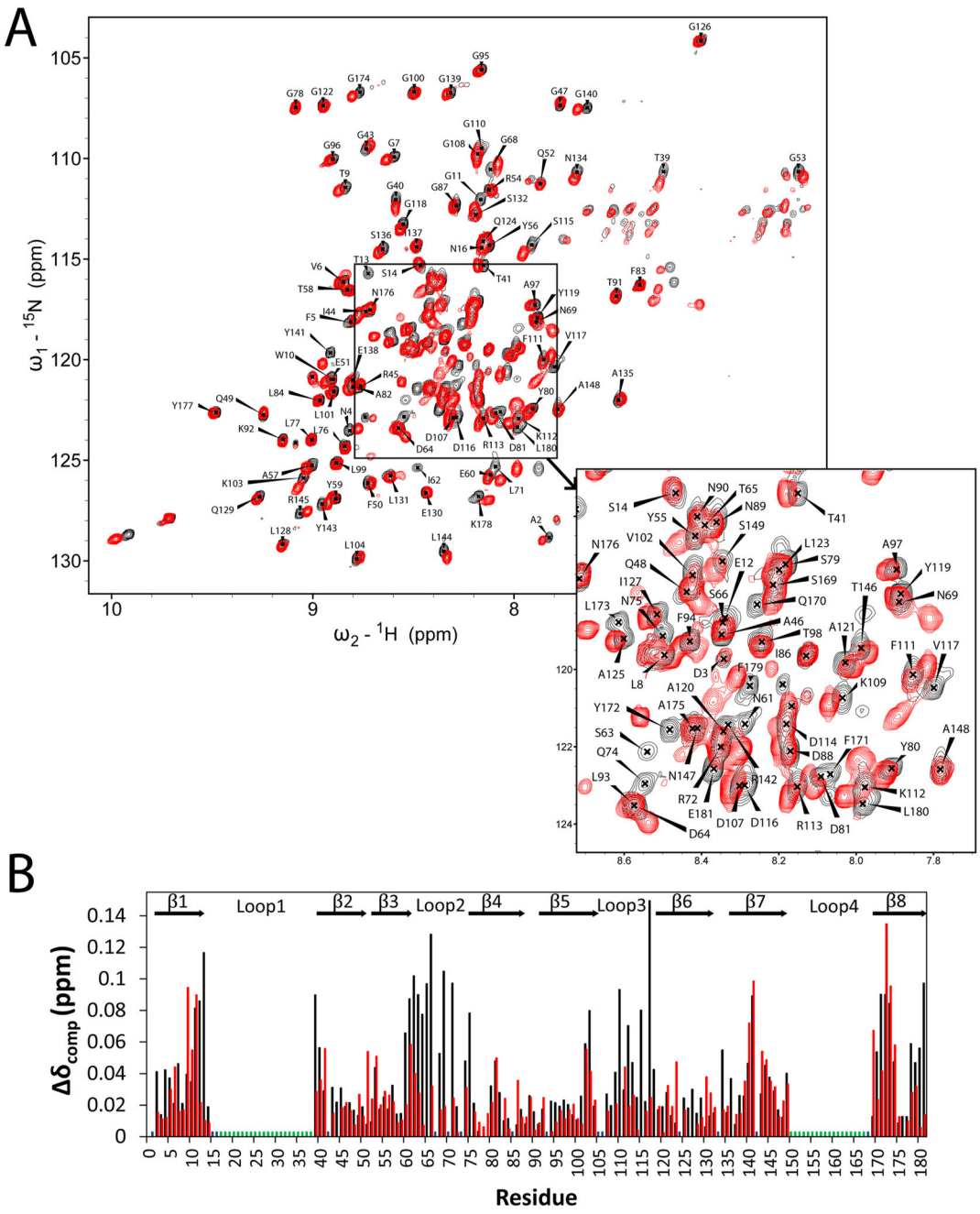

Figure 2.

Chemical shift perturbations in ^{15}N-^{1}H TROSY spectra upon addition of Kdo2-lipid A or LMPG to ^{2}H-,^{13}C-,^{15}N-labeled OprHΔL1ΔL4 in DHPC micelles. (A) ^{15}N–^{1}H TROSY spectrum of 0.2 mM OprHΔL1ΔL4 (black) in DHPC micelles overlaid onto the spectrum of OprHΔL1ΔL4 in DHPC:Kdo2-lipid A mixed micelles (red, 10:1 Kdo2-lipid A/OprH molar ratio). (B) Compound chemical shift changes $\Delta\delta_{comp} = [\Delta\delta^2_{HN} + (\Delta\delta_N/6.5)^2]^{1/2}$) resulting from the addition of 2 mM LMPG (red) and 2 mM Kdo2-lipid (black) relative to the chemical shifts of 0.2 mM OprHΔL1ΔL4 in DHPC only. Unassigned residues are marked with blue ticks, and removed loop residues are marked with green ticks.

Author Manuscript
Author Manuscript
Author Manuscript
Author Manuscript

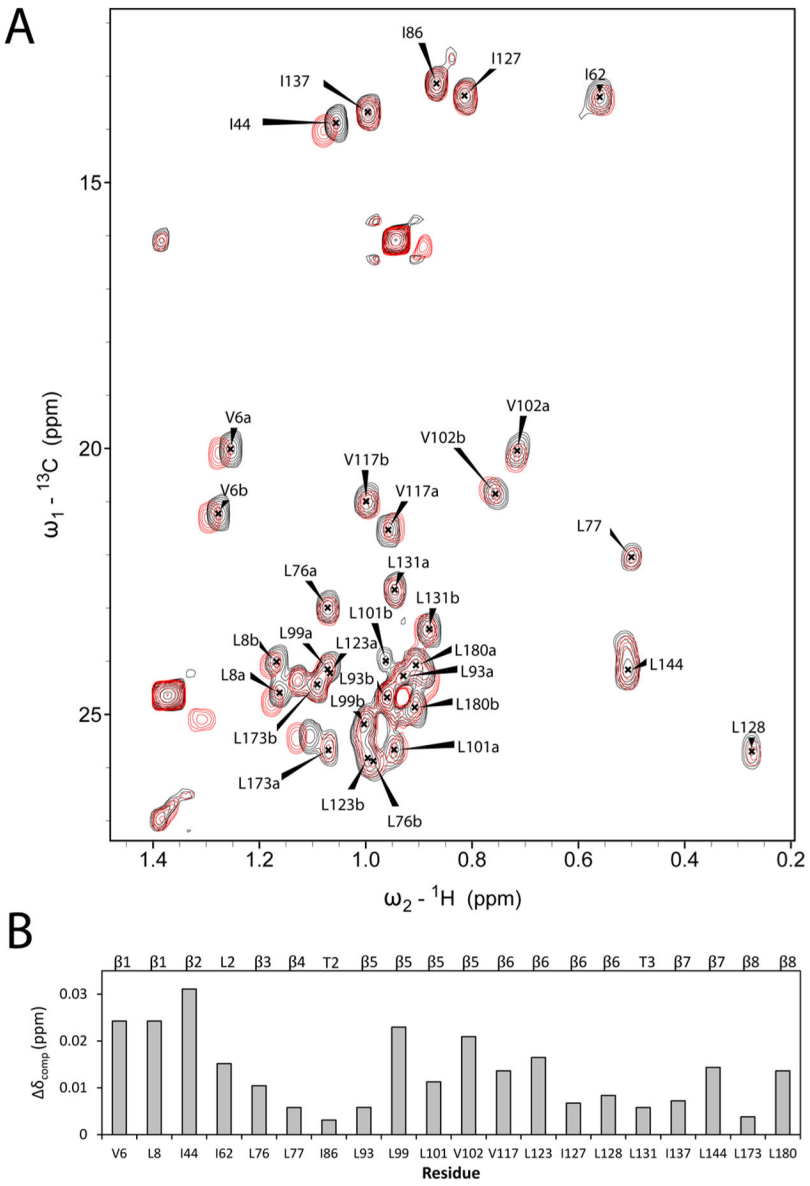

Figure 3.

Chemical shift perturbations in ^{1}H-^{13}C HMQC spectra upon addition of Kdo2-lipid A to {[U-^{2}H-, ^{15}N]; Ileδ1-[$^{13}CH_3$]; Leu,Val-[$^{13}CH_3$,$^{12}CD_3$]} labeled OprHΔL1ΔL4 in DHPC micelles. (A) ^{1}H–^{13}C HMQC spectrum of 0.5 mM OprHΔL1ΔL4 (black) in DHPC micelles overlaid onto the spectrum of OprHΔL1ΔL4 in DHPC/Kdo2-lipid A mixed micelles (red, 10:1 Kdo2-lipid A/OprH molar ratio). (B) Compound chemical shift changes $\Delta\delta_{comp} = [\Delta\delta^2_H + (\Delta\delta_C/5.4)^2]^{1/2}$) resulting from the addition of 2 mM Kdo2-lipid relative to the chemical shifts of 0.2 mM OprHΔL1ΔL4 in DHPC only.

Author Manuscript
Author Manuscript
Author Manuscript
Author Manuscript

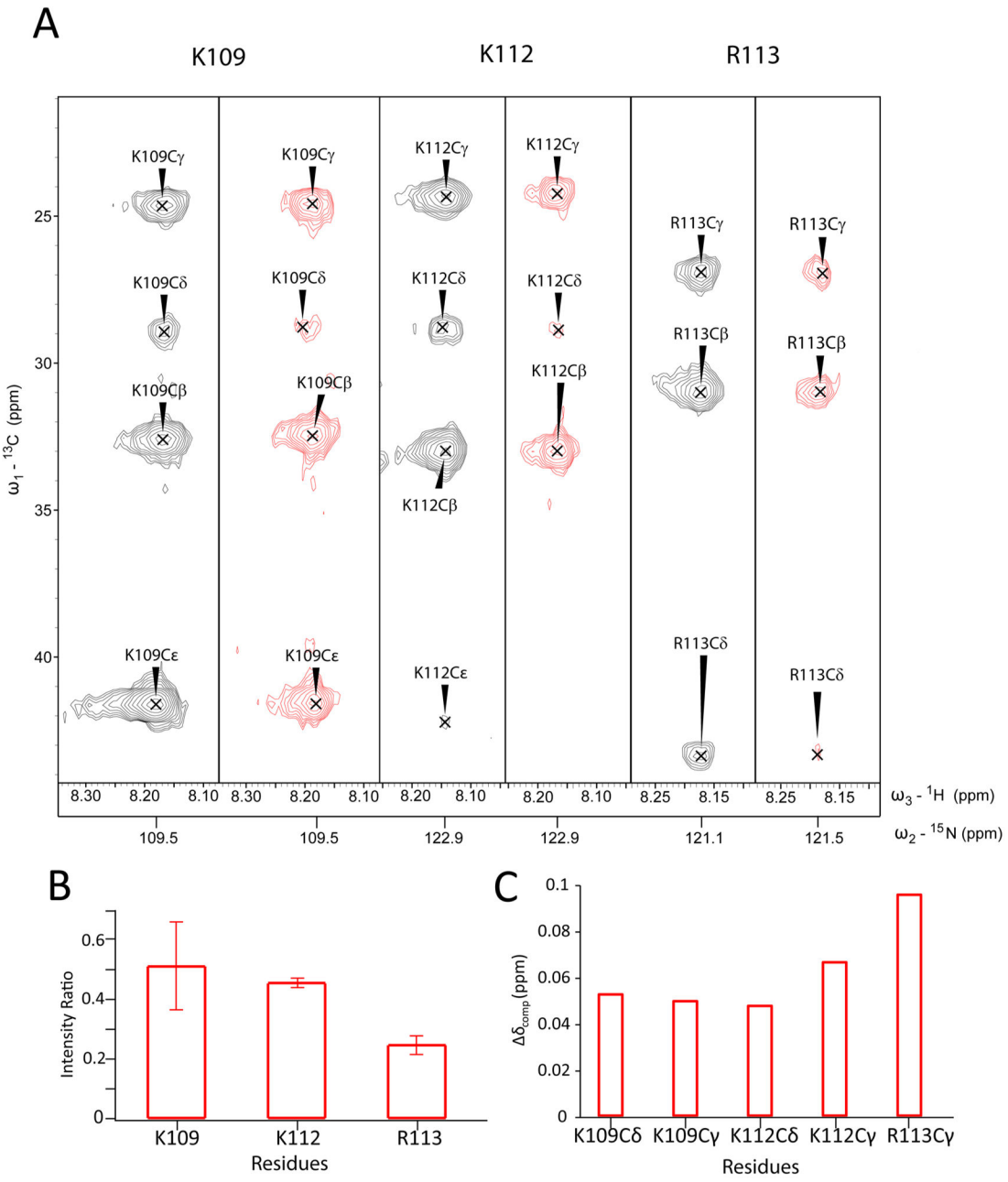

Figure 4.

Chemical shift perturbations in 3D H(C) (CC)-TOCSY-(CO)-[^{15}N,^{1}H]-TROSY spectra upon addition of Kdo2-lipid A to ^{13}C-,^{15}N labeled OprHΔL1ΔL4 in DHPC micelles. (A) [ω_1(^{13}C), ω_3(^{1}H)] strips from 3D H(C) (CC)-TOCSY-(CO)-[^{15}N,^{1}H]-TROSY spectrum of OprHΔL1ΔL4 in DHPC micelles (black) and ^{13}C-,^{15}N labeled OprHΔL1ΔL4 in DHPC:Kdo2-lipid A mixed micelles (red, 10:1 Kdo2-lipid A:protein molar ratio). The strips were taken at the ^{15}N chemical shifts indicated at the bottom of the strips. (B) Ratios of H(C) (CC)-TOCSY-(CO)-[^{15}N,^{1}H]-TROSY cross-peak intensities of the three charged loop 3 residues shown in panel A with and without Kdo2-lipidA. The values are the averages of

Author Manuscript Author Manuscript Author Manuscript Author Manuscript

the β, γ, δ, and (ε) position ratios, which were similar to each other for each residue, and the error bars are standard deviations. (C) Compound chemical shift changes $\Delta\delta_{comp} = [\Delta\delta^2_H + (\Delta\delta_N/6.5)^2 + (\Delta\delta_C/5.4)^2]^{1/2}$) resulting from the addition of 2 mM Kdo2-lipid relative to the chemical shifts of 0.2 mM OprHΔL1ΔL4 in DHPC only.

Author Manuscript Author Manuscript Author Manuscript Author Manuscript

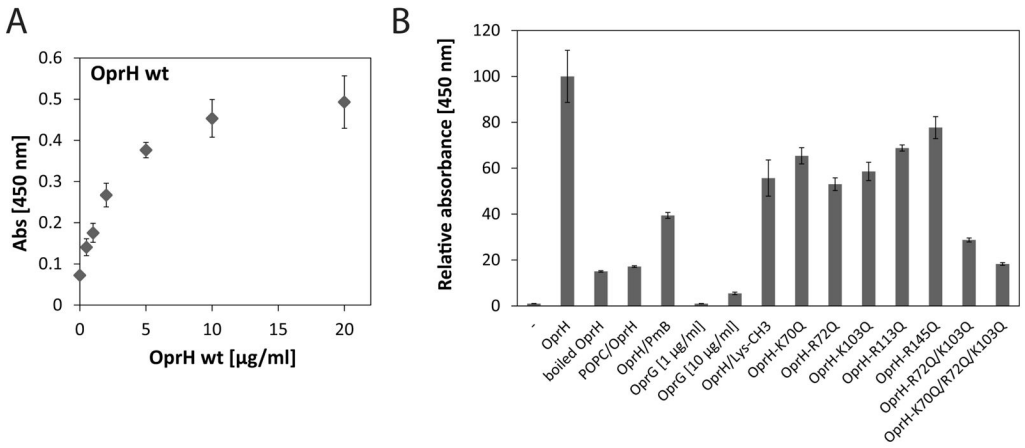

Figure 5.

Binding of OprH to LPS-coated surface. (A) Concentration dependence of OprH binding to LPS-coated microtiter plate. (B) Comparison of the binding of OprH and OprH mutants to LPS-coated microtiter plates. All proteins were used at 1 μg/mL concentration, with exception of OprG, which was used at both 1 and 10 μg/mL. "–" denotes no protein added, "POPC/OprH" – POPC was used to coat plates instead of LPS, "OprH/PmB" – after incubation with OprH, the plate was treated with 10 μg/mL polymyxin B for 30 min, "OprH/Lys-CH_3" – OprH with methylated lysine side chains was used, OprH-K70Q, -R72Q, -K103Q, -R113Q, -R145Q, -R72Q/K103Q, -K70Q/R72Q/K103Q – OprH mutants.

Author Manuscript
Author Manuscript
Author Manuscript
Author Manuscript

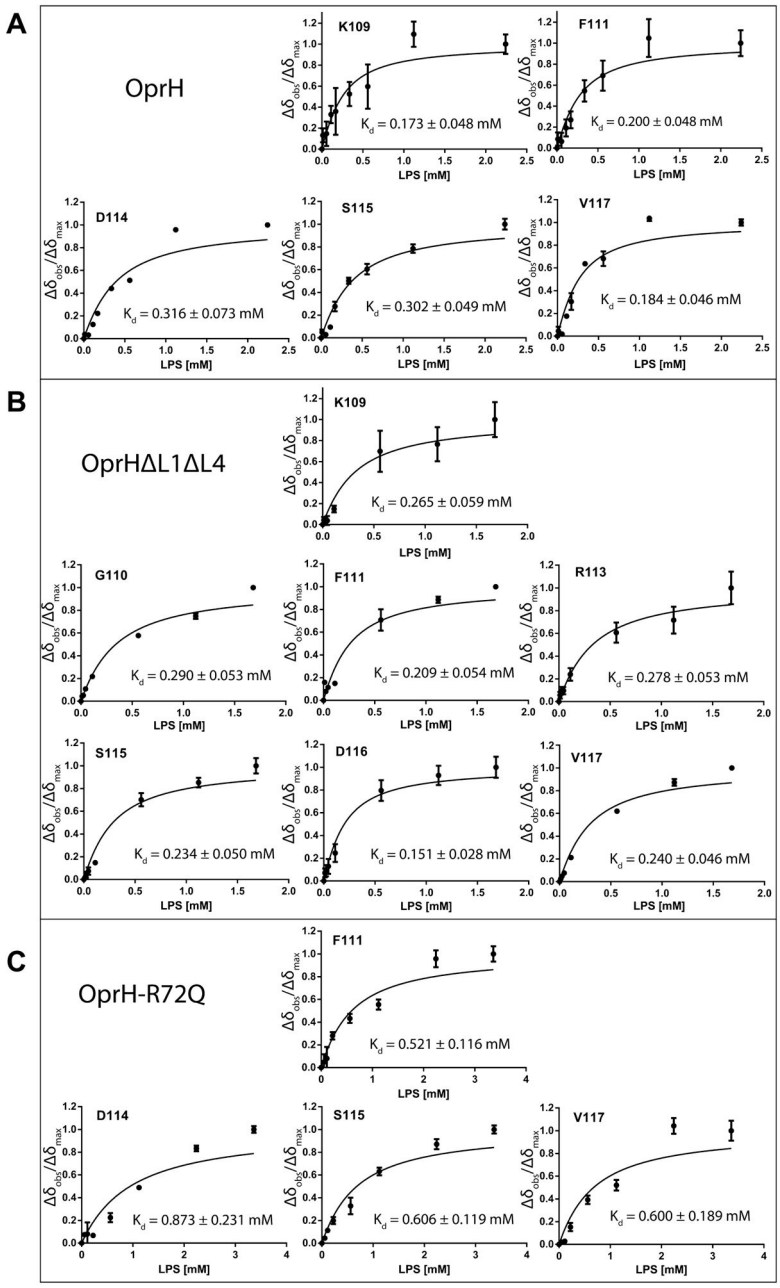

Figure 6.

Binding curves for Rd2 LPS binding to different forms of OprH using the $^{1}H_{N}$ chemical shift changes of selected loop 3 residues. (A) wt OprH, (B) OprHΔL1ΔL4, and (C) OprH-R72Q.